Automated Identification of Man-Made Textural Features on Satellite Imagery by Bayesian Networks

Ahmet B. Orun

Abstract

A classification technique which distinguishes between man-made and natural textural features visible on high resolution satellite images is introduced. The proposed work aims to evaluate non-linear classification techniques by the unification of appropriate texture analysis methods and a learning Bayesian classifier which is more robust against data uncertainty than the other types of linear classifiers. The classification technique introduced within this work will also provide an opportunity for fully automated thematic and land-use map generation.

Introduction

In the last few decades the use of satellite images in place of aerial photography has reduced the cost of map production by nearly a factor of six. One of the major issues in map production is the huge amount of visual data that has to be interpreted manually. For example a 5-meter-resolution satellite image approximately corresponds to a 1:25,000-scale map. For developing countries which have large land coverage (e.g., Sudan, Yemen, etc.), very large sets of maps at this scale need to be interpreted. This sort of manual interpretation should be done by highly qualified staff whereas these countries suffer from the lack of a sufficiently trained workforce and appropriate mapping equipment. The map revision procedure also requires visual interpretation and should be repeated regularly to include the latest available data due to expansion of urban areas, natural land changes, etc. Sometimes it may be difficult to distinguish between natural textural features and poorly structured residential areas, especially in city suburbs. In such cases the classifier proposed in this work will operate as a decision support system (DSS) for map generation which distinguishes between very similar terrestrial features. The proposed method may also contribute to fully or semiautomated mapping procedures, especially for developing countries where manual inspection is much more difficult.

Machine learning (ML) and data mining (DM) techniques have been used effectively in the last decade for aerial image interpretation and geographic feature classification. Sung and Pachowiez (2002) developed an adaptive object recognition technique which uses texture-based image analysis for detection and tracking of geographical features on images. The method is used for segmentation of textural features on the image by integration of Gabor filters, Laws' energy filters, and modified radial basis function classifiers. It may be concluded from the experiments that the method may only be used to classify very distinguishable textural features. Pesaresi and Benediktsson (2000) investigated feature extraction by classification of panchromatic high-resolution satellite image data from urban areas using neural networks. As is well known, neural networks, unlike Bayesian networks, cannot build relationships between all variables in the network. Geman and Jedynak (1996) introduced an active testing model for tracking roads on satellite images. The method is based on a statistical model, including joint distribution and an on-line decision tree. Nilubol *et al.* (2002) used synthetic aperture radar (SAR) images to classify the targets using Hidden Markov Models. The method was developed as an alternative to template matching, and ten different target classes were used. In Rellier *et al.* (2002), a Bayesian approach was used to specify local registration and deformation of a road cartographic network on a satellite image to avoid differences between the map data and ground truth.The method does not work with textural features.

Even though there are some similarities between these methods and our proposed method, our method differs in terms of a specific unification of Bayesian classifiers and a textural analysis technique which is described in the next section. The method also shows similarity with one which was previously presented by Orun and Alkis (2003) on the identification of different materials.

The main objective of the proposed method is to gain the highest accuracy of textural feature classification on the satellite images by using an automatic operation and a single image band to reduce the data and labor cost. Multispectral data would increase the labor and computational cost but would not make too much contribution to the textural analysis result. This is based on the assumption that textural content remains almost the same in different bands. The final classification results obtained fall into two categories: (1) classification of two textural classes (man-made and natural) and (2) classification of six textural classes (four man-made and two natural).

Techniques Used

Data Acquisition and Specification

Image samples of the texture classes used in the experiments were extracted from a large digital satellite image of the Izmir area in Turkey acquired by an environmental satellite from an approximate altitude of 817 km. The satellite sensor (IRS-1) provides a 5-meter resolution panchromatic (photographic)

School of Computer Science, University of Birmingham, Birmingham, United Kingdom (A.B.Orun@cs.bham.ac.uk). aboIL@onetel.net.uk

Photogrammetric Engineering & Remote Sensing
Vol. 70, No. 2, February 2004, pp. 211–216.

0099-1112/04/7002–0211/$3.00/0

image with about a 75- by 75-km ground coverage. The image data contains 256 grey levels (8-bits per pixel). The imagery at this scale was selected because of its compatibility with the 1:25,000-scale thematic mapping experiments.

Texture Analysis

Texture analysis algorithms have been comprehensively studied by several authors (Greenspan, 1994; Rushing *et al.*, 2001; Ayala, 2001). They are also frequently used to identify textural features visible on aerial or satellite images (Ionescu, 1989). It is widely accepted that textures can be classified into two main categories: structured and unstructured (stochastic) forms. The textures visible on high-resolution satellite imagery or aerial photography may often fall into the second category where no specific rule may be applied to specify the characteristics of the texture primitives. There exist a few methods to extract textural features such as structural, statistical, or spectral properties. The techniques based on grey-level co-occurrence statistics (Haralick, 1979), grey-level run-length statistics (Chu *et al.*, 1990), texton gradiens (Julesz, 1986), Gabor filters (Jain and Karu, 1996), and random field models (Wu and Doerschuk, 1994) are the best known. In this work, five statistical measures were used (derived from Phillips (1995)) in order to specify each texture's statistical characteristics. Two different sizes of operation windows (3 by 3 and 5 by 5) were used for Equations 1 through 4 and a 3 by 3 window size for Equation 5. Large window sizes produce large edge effects at the class edges but provide more stable texture measures than do small windows. In return, a small window size is less stable but has a smaller edge effect (Christopher and Warner, 2002).

$$Variance_{Russ} = \sqrt{\sum (centerpixel - neighbor)^2} \quad \text{(Russ)} \quad (1)$$

$$Variance_{Levine} = \frac{1}{area} \sum (centerpixel - mean)^2 \quad \text{(Levine)} \quad (2)$$

$$\sigma = \sqrt{Variance_{Levine}} \quad \text{(Sigm)} \quad (3)$$

$$Skewness = \frac{1}{\sigma^3} \frac{1}{area} \sum (centerpixel - mean)^3 \quad \text{(Skew)} \quad (4)$$

$$Std.\ Deviation = \sqrt{\frac{\sum (x - x')^2}{n}} \quad \text{(Stdev)} \quad (5)$$

In Equation 1, "centerpixel" denotes the intensity of a pixel in the middle of a window and "neighbor" denotes an intensity value for each pixel in the window. In Equation 2, "area" corresponds to the size of the window (9 for a 3 by 3 window size). The average pixel intensity value in a window is denoted as "mean" and also shown as x' in Equation 5.

Because the variance of the Russ method is independent from the size of the sample area (Figure 1), it allows for free sampling of the classes in an image. However, the other methods require sampling always at the same area size. Equations 1 through 5 denote the pixel-based statistical feature extraction from the sample images which are shown in Figure 1. Here, selected samples represent man-made features (rows between "a" and "d") and natural features (rows between "na" and "nb") on high-resolution satellite images.

Bayesian Networks

Bayesian Networks (BN) are known as "directed acyclic graphs" (DAG) which perform knowledge representation and reasoning even under uncertainty. They are also called directed Markov fields, belief networks, or causal probabilistic networks (Jensen, 1998). Bayesian networks are the probabilistic models which graphically encode and represent the conditional independence (CI) relationships among a set of data. In Bayesian networks each node represents a database attribute and is called a variable. The connections (arcs) between the nodes represent dependency relationships of variables. Bayesian networks are very efficient tools for modeling the joint probability distributions of variables. For example, if $A = \{X_1, \ldots, X_n\}$ is a random variable which denotes patterns spanning the $n = N$ by M dimensional vector space, the joint

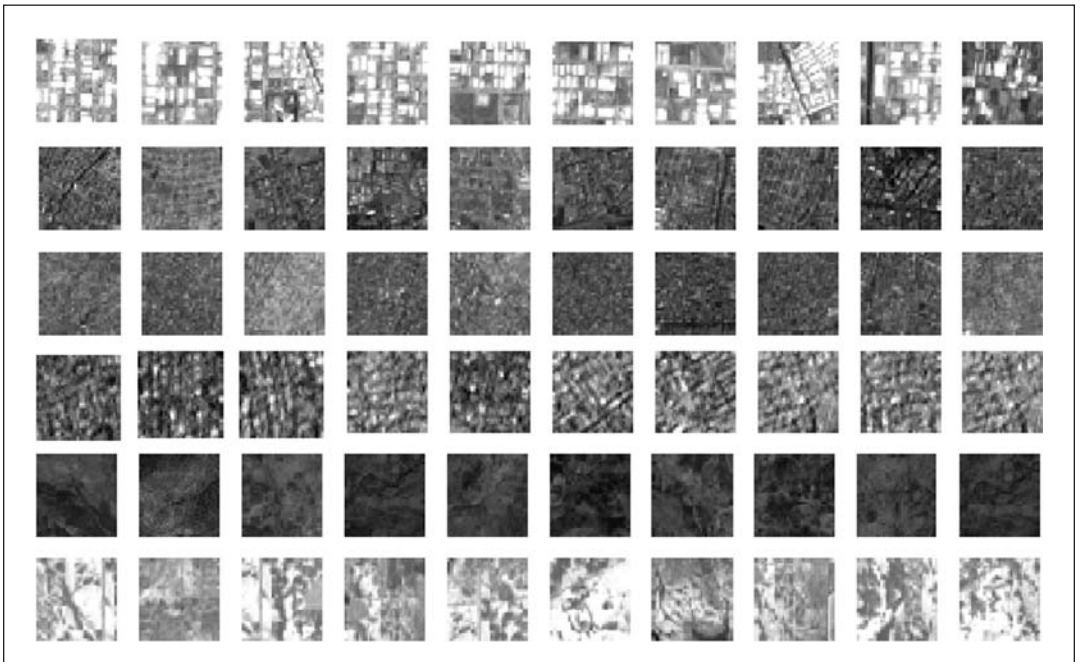

Figure 1. Selected samples representing man-made textural features (rows: a-d) and natural textural features (rows: na-nb) on high resolution satellite images.

probability distribution $P = (X_1, \ldots, X_n)$ is then a product of all conditional probabilities and may be represented as

$$P(X) = \prod_i P(X_i \mid pa(X_i)). \quad (6)$$

In Equation 6 $pa(X_i)$ is the parent set of X_i. Structural learning is one of the major specifications of Bayesian networks. This is based on constructing relationships between the variables and is similar to the data mining principle. One of the major problems in the network is the automatic configuration of a correct causal structure of network variables. Structural learning algorithms are divided into two categories: (1) search and scoring based and (2) dependency analysis. In this work the second one is used to construct the network.

In this work a learning Bayesian Network software utility (PowerConstructor©) is used (Cheng *et al.*, 2002). The utility accepts continuous variables and uses the Markov condition to obtain a collection of conditional independence statements from the network (Pearl, 1988). All valid conditional independence relations can also be extracted from the topology of the network. The algorithm examines information regarding two related variables from a data set and decides if two variables are dependent. It also examines how close the relationship is between those variables. This information is called conditional mutual information of two variables X_i and X_j, which may be denoted as

$$I(X_i, X_j \mid C) = \sum_{x_i, x_j, c} P(x_i, x_j, \mathbf{c}) \log \frac{P(x_i, x_j \mid \mathbf{c})}{P(x_i \mid \mathbf{c}) P(x_j \mid \mathbf{c})}. \quad (7)$$

In Equation 7, C is a set of nodes and $\mathbf{c}$ is a vector (one instantiation of variables in C). If $I(X_i, X_j \mid C)$ is smaller than a certain threshold t, then we can say that X_i and X_j are conditionally independent. Selection of a threshold value in the software package is optional and may be between 0.1 and 50. The values $P(x_i, x_j \mid \mathbf{c})$ may be extracted from the conditional probability tables.

Conditional Independence

If there is a causal network with serial or diverging connections between the nodes A, B, and C ($A \rightarrow B \rightarrow C$ or $A \leftarrow B \rightarrow C$), then A and C are conditionally independent if evidence is inserted into node B. In this case, C does not effect A due to independence.

The variables A and C are independent, given the variable B, if:

$$P(a_i \mid b_j) = P(a_i \mid b_j, c_k) \quad \text{for all } i, j, k \quad (8)$$

(note that a_i, b_j, c_k are the states of A, B, C).

If we redefine Equation 8 by the conditioned Bayes Rule, then

$$P(A \mid B, C) = \frac{P(C \mid A, B) P(A \mid B)}{P(C \mid B)} = \frac{P(C \mid B) P(A \mid B)}{P(C \mid B)} = P(A \mid B). \quad (9)$$

In Equation 9, the proof requires that $P(C \mid B) > 0$ (Jensen, 1998).

Numerical Results

Selection of Data Sets

For the classification experiments, six classes were specified from residential, mountainous, and sea coast areas. For each class, ten sample regions were selected (Figure 1). All samples for a given texture classes were extracted from a large digital satellite image. Each sample had a size of 35 by 35 pixels, each with 256 grey-level values. The textural features of each sample were extracted using five different texture analysis measures (Equations 1 through 5). The analyses were carried out by scanning with 3 by 3 and 5 by 5 operational windows over the sample image. The first half of the results (first 30 cases) was used as the set for network training and the second half (second 30 cases) was used as the test set. This ideal ratio of 1:1 between training/test sets had been decided by the experiments. The numerical values of statistical textural measures (extracted from the sample images) are shown in Table 1 (for urban1 and urban2) and in Table 2 (for natural features). They were both included in the training set.

TABLE 1. THE RESULTS OF TEXTURE ANALYSES FOR TWO SAMPLE CLASSES FROM URBAN AREAS

Image	Russ1	Levine1	Sigm1	Skew1	Russ2	Levine2	Sigm2	Skew2	Stdev	Class
a1	322	589	24.3	1.9	154	583	24	0.6	40	urban1
a2	550	642	25	2	200	714	27	−0.2	47	urban1
a3	426	744	27.3	1.6	197	818	29	0.3	42	urban1
a4	441	762	27.6	1.4	364	861	29	0.2	42	urban1
a5	172	622	25	1	95	1045	32	0.7	45	urban1
b1	139	336	18.3	1.2	79	356	19	0.4	23	urban2
b2	204	443	21	1.2	179	576	24	1.1	29	urban2
b3	175	275	16.6	1	79	280	17	0.4	19	urban2
b4	354	315	17.7	1.9	110	278	17	0.7	22	urban2
b5	259	289	17	1.1	78	324	18	0.6	21	urban2

TABLE 2. THE RESULTS OF TEXTURE ANALYSES FOR TWO SAMPLE CLASSES FROM NATURAL AREAS

Image	Russ1	Levine1	Sigm1	Skew1	Russ2	Levine2	Sigm2	Skew2	Stdev	Class
na1	201	106	10.3	1.6	89	109	10	0.3	17	nature1
na2	210	131	11.4	1.7	77	122	11	0.4	16	nature1
na3	154	116	10.8	1	77	155	12	0.4	17	nature1
na4	117	92	9.6	1.9	50	76	8.7	−0.1	14	nature1
na5	112	71	8.4	1.6	38	72	8.5	0.1	12	nature1
nb1	356	556	24	2	206	529	23	−0.1	34	nature2
nb2	320	410	20	2	68	394	20	0.2	34	nature2
nb3	338	568	24	1.5	226	707	27	0.1	40	nature2
nb4	346	306	17.5	2.6	75	208	14	0.2	24	nature2
nb5	334	497	22	1.8	125	536	23	−0.3	36	nature2

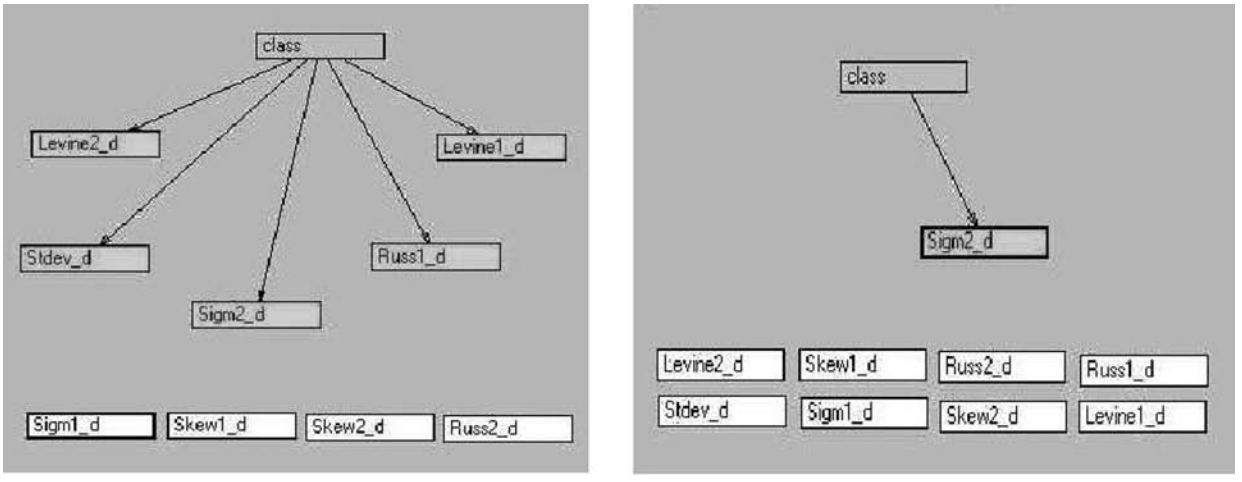

(a) (b)

Figure 2. Automatically selected nodes of the networks are shown in a graphical form displayed by the Bayesian classifier (Powerconstructor®) after the training process. The figures show two different tests. (a) Using six classes. (b) Using two classes.

Classification

Suitable system parameters such as the discretization interval value (δ) which is used for slicing the continuous variables, the discretization method, the threshold value (t) to specify the conditional independence between variables, etc. should be selected during the network training and classification process. After experiments, δ was selected to be as high as possible (30) for maximum accuracy, the "Equal frequency" method was used for the discretization of continuous variables, and t was selected to be as small as possible (0.1) in order to improve the training accuracy. We have to note that, if t is selected smaller than that, then the model becomes more complex and the test accuracy decreases. There are no certain rules for selecting the system parameters (e.g., t, δ). They can only be optimized by experimentation, depending on the field of application.

The training of the network was the first step in the classification process. After the training stage, conditionally dependent nodes (variables) were connected to each other by the conditional independence (CI) rules as described earlier in the section on Bayesian Networks. Two kinds of classification tests were performed (Figure 2). First, two classes (man-made and natural textures) were specified, and second, six classes (four residential and two natural areas) were specified. The graphical displays of the results are shown in Figure 2. The class node (class) is connected to some of the variables which contain different textural analysis measures. Here the class node represents the "identification" of textural features. Other nodes which have no connection are not necessarily unimportant but their connection would not make any additional contribution to the results. Because no connection was established between the nodes of Russ, Levine, etc., a conclusion could be made that there is no cause-effect relationship between two nodes or that such a connection between the nodes might be ignored by the system (as between the Sigm and Levine nodes in Figure 2) in order to optimize the network so that it gains maximum classification accuracy. This is because the first priority in the network construction is given to classification accuracy rather than showing the dependencies between the nodes.

Because the Bayesian classifier has a probabilistic nature of calculation, an increase in the number of system variables, will cause the number of calculations to increase exponentially. Too many variables may also cause an overfitting problem. To avoid such shortcomings in this work, only five texture analysis measures were used. The whole classification procedure is described in Figure 3, and the results of accuracy and class-confusion matrices are summarized in Tables 3, 4, and 5.

Automatic Mapping Procedure

The classification techniques described earlier were applied to one image layer for the mapping experiment. To achieve this, five test sites were selected manually (from one natural

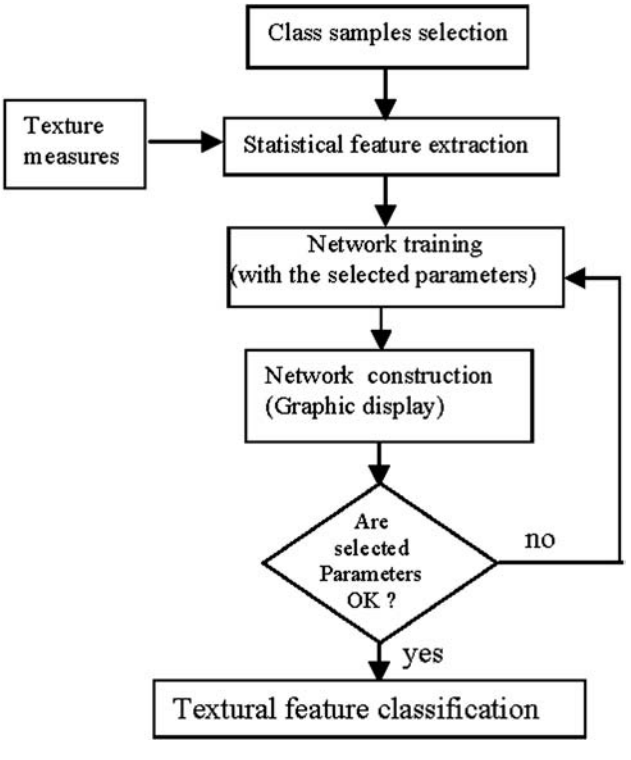

Figure 3. Flow chart of the classification process.

TABLE 3. CLASS CONFUSION MATRIX OF CLASSIFICATION RESULTS FOR DIFFERENT TEXTURAL FEATURES

Class-confusion matrix-I

Values (%)	Urban 1	Urban 2	Urban 3	Urban 4	Natural1	Natural2
Urban 1	60	0	0	20	0	20
Urban 2	0	80	0	20	0	0
Urban 3	0	20	80	0	0	0
Urban 4	0	0	0	80	0	20
Natural1	0	0	0	0	100	0
Natural2	40	0	0	20	0	40

TABLE 4. CLASS CONFUSION MATRIX OF CLASSIFICATION RESULTS FOR MAN-MADE AND NATURAL TEXTURAL FEATURES

Class-confusion matrix-II

Values (%)	Urban (man-made) Texture	Natural Texture
Urban (man-made) texture	100	0
Natural texture	40	60

and four urban areas), each one consisting of test frames. Each test frame in the sites was subjected to statistical texture analysis and classification.

When choosing the size of the test frames, we needed to consider the contradictory requirements of the two following conditions:

- Each test frame should be large enough to cover a sufficient amount of texture primitives. This will provide a stable texture measure for texture analysis. This condition is more difficult to achieve in natural areas where the texture primitives are quite large and unstructured.
- Test frame size, on the other hand must be small enough to avoid edge effects (as indicated by Christopher and Warner (2002)). Especially for fractured areas or at class boundaries, a large frame size will cause multiple class selection. We have to note that we cannot select different sizes of frames to suit different ground features. Due to the high correlation between the size and texture measures of a frame, all frames must be at the same size for an exact comparison of the textural numerical results.

TABLE 5. CLASSIFICATION ACCURACY RESULTS FOR TWO DIFFERENT CATEGORIES (FOR TWO AND SIX TEXTURAL CLASSES WITH DIFFERENT DISCRETIZATION METHODS)

Classification accuracy results (at 95% confidence level)

Number of classes included into the classification procedure	Classification results after discretization by maximum entropy	Classification results after discretization by equal frequency
Man-made and Natural textures (2 classes)	83.3% ± 13.34%	86.7% ± 12%
Man-made (4) and Natural textures (2) (6 classes)	73.3% ± 15.82%	66.7% ± 16.9%

The statistical features which were extracted from these sites by the texture measures (described in the section on Texture Analysis) were used as a test set for Bayesian classifiers. On the satellite image, two areas of different classes were separated by a boundary which was delineated by an expert (shown in Figure 4). According to the results presented in Table 6, the overall accuracy of textural feature identification

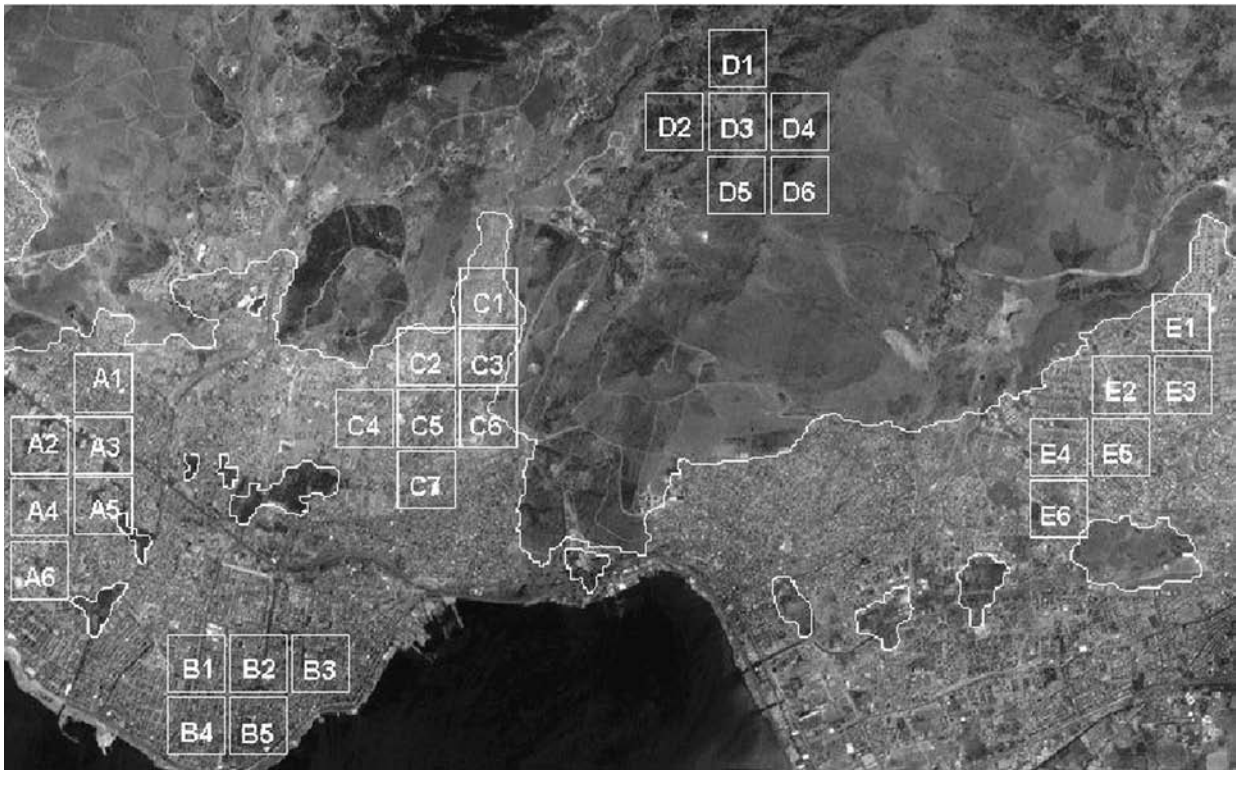

Figure 4. The test sites where the proposed automatic map generation technique was applied. The boundary between two different textural classes (man-made and natural) was delineated by a mapping expert.

TABLE 6. THE RESULTS OF TEXTURAL FEATURE IDENTIFICATION ON THE TEST AREAS IN FIGURE 4 (M = MAN-MADE, N = NATURAL)

Area	Output	Prob. Man-Made	Prob. Natural	Results
a1	M	0.65	0.35	TRUE
a2	M	0.65	0.35	TRUE
a3	N	0.07	0.93	FALSE
a4	M	0.93	0.07	TRUE
a5	M	0.93	0.07	TRUE
a6	M	0.93	0.07	TRUE
b1	M	0.93	0.07	TRUE
b2	M	0.93	0.07	TRUE
b3	M	0.93	0.07	TRUE
b4	M	0.93	0.07	TRUE
b5	N	0.07	0.93	FALSE
c1	M	0.65	0.35	TRUE
c2	M	0.93	0.07	TRUE
c3	M	0.65	0.35	TRUE
c4	M	0.93	0.07	TRUE
c5	M	0.65	0.35	TRUE
c6	M	0.65	0.35	TRUE
c7	M	0.93	0.07	TRUE
d1	N	0.07	0.93	TRUE
d2	N	0.07	0.93	TRUE
d3	N	0.07	0.93	TRUE
d4	N	0.07	0.93	TRUE
d5	N	0.07	0.93	TRUE
d6	N	0.07	0.93	TRUE
e1	M	0.93	0.07	TRUE
e2	M	0.93	0.07	TRUE
e3	M	0.65	0.35	TRUE
e4	M	0.65	0.35	TRUE
e5	N	0.07	0.93	FALSE
e6	M	0.65	0.35	TRUE

at the selected test sites was 90 percent. This was especially higher for the natural region.

We have to note that the automatic map generation results presented in this section give an approximate idea of mapping accuracy. For a complete mapping procedure, the size of test frames ($a_i, \ldots, e_i$) would be optimized further, as was mentioned earlier. At the class boundaries, where the test frame contains more than one class, some additional techniques (such as sub-pixel definition) would be used to separate the sub-classes.

Conclusion

In the geographic mapping industry, thematic maps play a vital role in urban planning and land-use strategy definition. In extreme cases, when quick decisions are to be made on urban and land-use planning by the use of appropriate map layers, difficulties can be faced to complete a thematic map series of large areas in a short time. The algorithms proposed within this work aim to overcome these kinds of difficulties and may lead to fully automatic mapping by the use of *Machine learning* techniques and learning classifiers. Bayesian learning classifiers are especially useful for overcoming uncertainties contained in satellite image data, which may cause differences between the map and ground truth.

Only five textural measures were used within the proposed work which were previously tested on unstructured textures (e.g., garment, wood, etc.) and yielded good results. However, some other texture analysis measures (such as energy, entropy, etc.) should also be included and tested for a trade-off.

The objective of the work in terms of accuracy has been achieved for the first category of results, which included only two single classes (man-made and natural) yielding 86.7 percent classification accuracy, whereas the second category (containing six classes) provided a much lower accuracy (73.3 percent).

Acknowledgment

I would like to thank Mark O'Dwyer for his generous contribution and constructive criticism.

References

Ayala, G., and J. Domingo, 2001. Spatial size distributions: applications to shape and texture analysis, *IEEE Transactions on Pattern Analysis and Machine Intelligence*, 23(12):1430–1442.

Cheng, J., D. Bell, and W. Liu, 2002. *Learning Bayesian Networks from Data: An Efficient Approach Based on Information Theory*, http://www.cs.ualberta.ca/~jcheng/lab.htm (link to report98.pdf), last accessed 06 November 2003).

Christopher, J.S., and T.A. Warner, 2002. Scale and texture in digital image classification, *Photogrammetric Engineering & Remote Sensing*, 68(1):51–63.

Chu, A., C.M. Sehgal, and J.F. Greenleaf, 1990. Use of grey value distribution of run lengths for texture analysis, *Pattern Recognition Letters*, 11:415–420.

Geman, D., and B. Jedynak, 1996. An active testing model for tracking roads in satellite images, *IEEE Transactions on Pattern Analysis and Machine Intelligence*, 18(1):1–13.

Greenspan, H., R. Goodman, R. Chellappa, and C.H. Anderson, 1994. Learning texture discrimination rules in a multiresolution system, *IEEE Transactions on Pattern Analysis and Machine Intelligence*, 16(9):894–901.

Haralick, R.M., 1979. Statistical and structural approaches to texture, *Proceedings IEEE*, 67(5):786–804.

Ionescu, D., 1989. A 2-D least square estimation method for texture extraction in aerial images, *Proceedings, International Geoscience and Remote Sensing Symposium, IGARSS'89, and 12th Canadian Symposium on Remote Sensing*, 10–14 July, Vancouver, British Columbia, Canada, 5:2794–2794.

Jain, A.K., and K. Karu, 1996. Learning texture discrimination masks, *IEEE Transactions on Pattern Analysis and Machine Intelligence*, 18(2):195–205.

Jensen, F., 1998. *An Introduction to Bayesian Networks*, Springer, New York, N.Y., 178 p.

Julesz, B., 1986. Texton gradients: The texton theory revisited, *Biological Cybernetics*, 54:247–251.

Nulibol, C., R.M. Mersereau, and M.J. Smith, 2002. A SAR target classifier using radon transforms and hidden markov models, *Digital Signal Processing*, 12:274–283.

Orun, A.B., and A. Alkis, 2003. Material identification by surface reflection analysis in combination with bundle adjustment technique, *Pattern Recognition Letters*, 24:1589–1598.

Pearl, J., 1988. *Probabilistic Reasoning in Intelligent Systems: Network of Plausible Inference*, Morgan Kaufmann, San Francisco, California, 552 p.

Pesaresi, M., and J.A. Benediktsson, 2000. Classification of urban high-resolution satellite imagery using morphological and neural approaches, *Proceedings, International Geoscience and Remote Sensing Symposium, 2000*, 24–28 July, Honolulu, Hawaii (IGARSS2000 and IEEE2000), 7:3066–3068.

Phillips, D., 1995. Image processing in C, Part15: Basic texture operation, *C/C++ Users Journal*, (November).

Rellier, G., X. Descombes, and J. Zerubia, 2002. Local registration and deformation of a road cartographic database on a SPOT satellite images, *Pattern Recognition*, 35:2213–2221.

Rushing, J.A., H.S. Ranganath, H.K. Hinke, and S.J. Graves, 2001. Using association rules as texture features, *IEEE Transactions on Pattern Analysis and Machine Intelligence*, 23(8):845–858.

Sung, W.B., and P.W. Pachowiez, 2002. Application of adaptive object recognition approach to aerial surveillance, *Proceedings of the Fifth International Conference on Information Fusion*, 08–10 July, Annapolis, Maryland (Air Force Office of Scientific Research), 1:658–663.

Wu, C., and P. Doerschuk, 1994. Texture based segmentation using Markov random fields, *Proceedings, Natural and Stochastic Methods in Image and Signal Processing III*, 28 July, San Diego, California (SPIE, Bellingham, Washington), 2304-16:86–93.